J Solid State Electrochem (1998) 2: 315–320

ORIGINAL ARTICLE

Dirk A. Fiedler

Rapid evaluation of the rechargeability of γ-MnO_2 in alkaline media by abrasive stripping voltammetry

Received: 25 November 1997 / Accepted: 20 January 1998

Abstract Cyclic abrasive stripping voltammetry is shown to provide the experimental basis for the evaluation of the rechargeability of γ-MnO_2 in 9 M KOH. Relative discharge capacities at different depths of discharge (DOD) with respect to the first one-electron reduction of γ-MnO_2 are compared when metal ions such as Ba^{2+} or Zn^{2+} are additionally present in the electrolyte solution. At about 30% DOD, resulting relative discharge capacities are essentially equal to those of AA cells either in the absence or presence of Ba^{2+} ions from about 10 discharge/charge cycles. However, the corresponding time scales are substantially different. While it takes about 2.7 h to complete 20 discharge/charge cycles in the case of abrasive stripping voltammetric characterization, some 360 h are needed to cycle an AA-sized battery in the conventional manner.

Key words Abrasive stripping voltammetry · Manganese dioxide · Rechargeable alkaline batteries · Rapid cycling

Introduction

The electroanalytical technique of abrasive stripping voltammetry (AbrSV) has been developed recently [1–4]. This method allows the study of solid particles when attached to an electrode surface after effectively polishing the electrode with the desired solid material. When applying this technique to manganese-based battery electrode materials such as $Li_xMn_2O_4$ or γ-MnO_2, values of peak potentials and, in case of $Li_xMn_2O_4$, also relative peak heights of voltammetric signals recorded within minutes were found to compare extremely well with those from long-term measurements at composite electrodes [5]. Similarly, in the case of doped electrolytic manganese dioxides, AbrSV was successfully employed as a rapid voltammetric screening method [6].

Since the invention of the rechargeable alkaline manganese dioxide (RAM^{TM}) cell, substantial work has been devoted to improving its rechargeability, and this has led to the successful introduction of such cells into the market place [7, 8].

The reduction or discharge of γ-MnO_2 may generally be described in terms of two consecutive one-electron processes I and II according to Eqs. 1 and 2 [7–9].

$$\text{Process I} \quad MnO_2 + H_2O + e^- \rightarrow MnOOH + OH^- \tag{1}$$

$$\text{Process II} \quad MnOOH + H_2O + e^- \rightarrow Mn(OH)_2 + OH^- \tag{2}$$

While Eq. 1 describes a homogeneous reduction step which occurs entirely in the solid state phase [9], Eq. 2 summarizes the dissolution of solid MnOOH to give $[Mn(OH)_6]^{3-}$, subsequent one-electron heterogeneous reduction to less soluble $[Mn(OH)_6]^{4-}$, and the final precipitation of $Mn(OH)_2$ [5, 7, 9]. Exhaustive indirect and direct evidence for the heterogeneous mechanism through dissolved intermediates can be found in notes [10, 11]. When γ-MnO_2 is reduced to the extent of up to approximately 50% with respect to Eq. 1, process I remains essentially chemically reversible. This effect is advantageously applied in RAM^{TM} cells [7, 8].

Basic cyclic abrasive stripping voltammetric behaviour of γ-MnO_2 in 9 M KOH electrolyte solutions where either the electrolyte solution or the MnO_2 itself contained different metal ions was described recently [6, 12]. In this work, the interaction of freshly immersed γ-MnO_2, when mechanically attached to an electrode surface, with metal ions such as Ba^{2+} and Zn^{2+} in aqueous 9 M KOH electrolyte solution is studied in more detail and on a significantly shorter time scale by cyclic abrasive stripping voltammetry. Multiple voltammetric

D.A. Fiedler (✉)
Institut für chemische Technologie anorganischer Stoffe,
Technische Universität Graz, Stremayrgasse 16/III,
A-8010 Graz, Austria
Tel.: +43-316-873 8288
Fax: +43-316-873 8272
e-mail: dirk.fiedler@munich.netsurf.de

cycling within pre-determined potential limits is applied in order to check for the reversibility of the discharge of γ-MnO_2. Resulting discharge curves are finally compared with those of AA-sized RAM^{TM} cells.

Experimental

Electrolyte solutions were prepared from KOH pellets (p.a., Merck, Germany) and deionized water. When desired, metal hydroxides $Ba(OH)_2 \cdot 8\ H_2O$ (p.a., Merck, Germany) or $Zn(OH)_2$ were added to saturation to freshly prepared 9 M KOH solutions. γ-MnO_2 (TOSOH Hellas, Greece; ≤90 μm, BET surface area 35 m^2/g) was transferred to a 0.5-mm diameter Pt disk electrode (Micro Glass Instruments, Australia) by effectively polishing this electrode with γ-MnO_2, causing some of the material to adhere to the electrode surface (Fig.1). Electrochemical studies were carried out under an Ar inert gas atmosphere in Ar-saturated electrolyte solutions with a three-electrode setup comprising the MnO_2-containing Pt disk working electrode and Hg/HgO (9 M KOH) reference and Pt mesh auxiliary electrodes. The electrochemical cell was controlled and data were collected by an IM5d impedance spectrometer (Zahner Elektrik, Germany) using the cyclic voltammetry software option. All potentials stated here refer to an Hg/HgO (9 M KOH) reference electrode when not stated otherwise.

For the determination of the amount of MnO_2 being attached to the surface of a 0.5-mm diameter Pt disk electrode, the procedure was as follows. Care was taken that MnO_2 particles adhered only to the Pt surface and not to the electrode body. After having recorded one voltammogram between −800 and 400 mV at 2 mV/s in the desired electrolyte solution, the material was dissolved in about 0.5 ml of concentrated hydrochloric acid (p.a., Merck, Germany) and brought to 2.0 ml with deionized water. Inductively coupled plasma (ICP) analyses were performed on such solutions for total manganese determination. Assuming that no material was lost during the voltammetric scan, the initial amount of γ-MnO_2 being attached to the electrode was calculated from background-corrected ICP analytical data.

Results and discussion

The quite hard and abrasive γ-MnO_2 was found to give lowest background currents when a glass-mounted Pt disk electrode was used rather than, e.g., a carbon electrode. No indication of any chemical or electrochemical interference between the electrode material and the studied γ-MnO_2 was evident. The BET surface area of about 35 m^2/g together with scanning electron microscopic photographs showed this material to be highly porous. Additionally, the studied material was found to be of fairly low crystallinity. Hence, for a successful AbrSV experiment, it is basically important to provide a good contact between the electrode surface and the γ-MnO_2. Because of the high inner surface area and low crystallinity, grain size distribution and particle shape were found to play a minor role in AbrSV studies on this type of γ-MnO_2. However, this may be peculiar to this material and needs to be individually checked for other materials which are neither so highly porous nor of such low crystallinity.

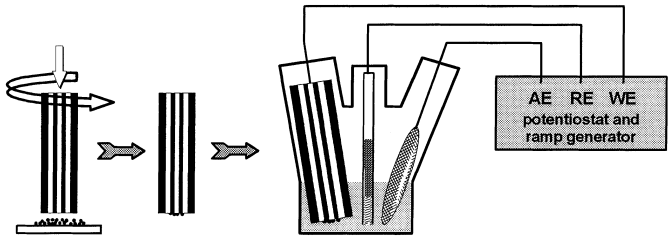

Fig. 1 Mechanical attachment of γ-MnO_2 to a Pt disk electrode and electrochemical cell assembly

Figure 2a shows the typical cyclic abrasive stripping voltammetric response of γ-MnO_2 in 9 M KOH. Process I as defined in Eq. 1 is observed in the potential range of 200 to −350 mV [5, 13–15], that is, between potentials E_0 and E_3. The voltammetric reduction response of this process appears to consist of multiple signals. Recent work divided the one process of Eq. 1 into three subprocesses [16–20], all of which take place in the solid state as far as manganese-containing species are concerned. Process II is then observed between −350 and −800 mV [5, 9, 13–15]. Upon oxidation, Mn-(III) species are generated in the −300 to 0 mV region, and formation of δ-MnO_2 takes place at about 350 mV [14]. The second voltammetric cycle clearly shows an additional signal at −400 mV when compared to the first one. This signal is attributed to the reductive generation of Mn_3O_4 from δ-MnO_2 [14].

Since in the technique of cyclic voltammetry there is a linear change of potential with time, this being excitation signal, the potential axis simultaneously represents a linear time axis. When integrating the current over time between $t(E_0)$ (E_0 = 170 mV) and $t(E_3)$ (E_3 = 350 mV), we can define a charge value for full one-electron discharge under potentiodynamic conditions. Typical resulting values are in the range of −250 to −300 μA s, which corresponds to the reduction of 2.5 to 3.0 nmol or 225 to 270 ng of γ-MnO_2 according to Faraday's law. Specific discharge capacity values of three independent AbrSV experiments from such integrations are compared with ICP analytical data in Table 1. The three samples of γ-MnO_2 were dissolved after having recorded a full voltammetric cycle encompassing both reduction processes I and II and subsequent oxidation processes, which mostly lead to the generation of δ-MnO_2 as outlined above. Therefore, irreversible loss of material due to dissolution of products is assumed to be negligible on the voltammetric time scale. As a result, from these ICP determinations, about 10% of the γ-MnO_2 attached to the electrode is voltammetrically accessible, which gives an idea of material usage in this specific case, which can be related to the poor conductivity of γ-MnO_2 [9]. Specific discharge capacities are thus of the order of 30 mA h/g. Such values, which were derived from AbrSV measurements, are comparable with those of high-rate alkaline manganese dioxide battery discharge tests [8], where also only a fraction of the available γ-MnO_2 is discharged [8, 9].

Partial reduction or discharge is accordingly defined by switching the potential anywhere between the rest

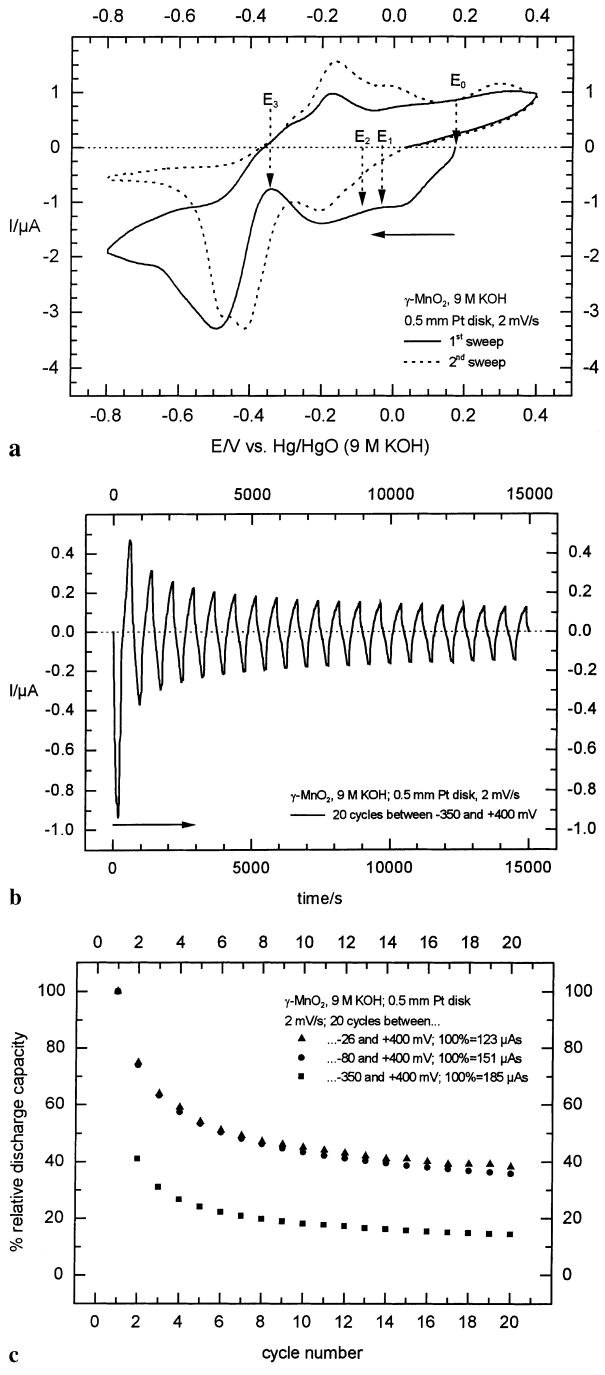

Fig. 2 **a** Cyclic abrasive stripping voltammetry of γ-MnO_2. Scan direction as indicated by solid arrow. Rest potential E_0 and various switching potentials E_1 to E_3 are indicated by *dotted arrows*. **b** Successive abrasive stripping voltammetric cycles of γ-MnO_2. Cycles started at rest potential E_0 and were continued between switching potentials $E_3 = -26$ mV and $E_4 = 400$ mV. Charge values for reduction (discharge capacities) and oxidation (charge capacities) were determined by integrating this current response over time between points of zero current. **c** Relative discharge capacity of γ-MnO_2 for various switching potentials as calculated from integrated data sets analogous to that of Fig. 2c. Values corresponding to each 100% discharge capacity are indicated

potential and that resembling full one-electron discharge under conditions of AbrSV. By dividing the charge value of partial reduction or discharge by that of full discharge, we can calculate the depth of discharge (DOD). Figure 2b shows the current response over time at 100% DOD, corresponding to repetitively reducing and oxidizing surface-attached γ-MnO_2 in the potential range -350 to 400 mV. Integration of intervals between adjacent points of zero current leads to values of discharge (integration of reductive currents) and charge (integration of oxidative currents). Taking the first discharge value as 100%, relative discharge capacities are calculated by dividing each subsequent discharge capacity value by that of the very first. Resulting graphs are displayed in Fig. 2c for 100%, 40% and 30% DOD, corresponding to potential ranges of -350, -80 and -26 mV to 400 mV, respectively. The time scale for such experiments varies between 4.2 and 2.7 h, depending on the chosen switching potentials at a voltammetric scan rate of 2 mV/s. While the difference in cycle lives between 30 and 40% DOD is insignificant in this electrolyte system, more than half of the initially available MnO_2 is used up after the seventh cycle under these conditions. When discharging to 100% with respect to Eq. 1, less than a fifth of the MnO_2 can be re-oxidized and used for further cylces [7]. In this latter case, and in contrast to a DOD of 30 or 40% (cf. the discussion of the reaction mechanism of process I above), some irreversible loss of MnOOH due to dissolution reactions can be anticipated in accordance with Eq. 1 and the mechanism leading to process II. However, this would also occur in a real RAM^{TM} cell to a significant extent under such discharge conditions, and is thus believed not to dramatically affect any comparison between AbrSV and real battery data. Note that this irreversible loss due to dissolution is possible, since, when switching the potential at about -350 mV, oxidative currents and thus oxidative formation of solid phases of MnO_2 are first observed about 150 s later. However, when further scanning towards negative potentials, process II with eventual generation of solid $Mn(OH)_2$ immediately follows initial dissolution of MnOOH (see Fig. 2a). Therefore, irreversible loss due to dissolution of Mn(III) species is considered to be insignificant when a complete 2-electron electrochemical reduction of γ-MnO_2 is performed, and could occur to an unknown (yet assumed to be negligible) extent under conditions of a full one-electron reduction because of the potentiodynamic boundary conditions employed.

We now consider the case of Ba^{2+}-saturated 9 M KOH electrolyte solution. The interaction between partially reduced γ-MnO_2 and Ba^{2+} generally enhances the rechargeability of γ-MnO_2 in RAM^{TM} cells, and this effect has been reported earlier [7, 21]. However, voltammetric evidence was then unavailable. Figure 3a clearly shows a diminished abrasive stripping voltammetric response of process II as defined in Eq. 2, which may simply be interpreted in terms of reduced solubility of intermediate $[Mn(OH)_6]^{3-}$ in the presence of Ba^{2+} ions.

Table 1 ICP analytical data of dissolved γ-MnO_2 which was attached to the surface of a 0.5-mm diameter Pt disk electrode and subjected to one voltammetric cycle between 800 and −400 mV prior to dissolution in HCl and dilution to 2.0 ml. Data shown are of three independent AbrSV experiments of the same γ-MnO_2 (TOSOH, Greece). Charge values $-Q_{CV}$ were calculated from the voltammograms by integrating the current response over time in an interval enclosed by E_0 and E_3 = −350 mV

γ-MnO_2 exp.no.	$c(Mn)_{corr}$[a] [µg/l]	$M(MnO_2)_{corr}$[b] [µg]	$-Q_{CV}$ [µA s]	$-Q_{CV}/M(MnO_2)_{corr}$ [mA h/g]	Fraction[c] [%]
1	765	2.42	262	30.1	9.8
2	605	1.92	299	43.3	14
3	1170	3.70	294	22.1	7.2

[a] All measured values are corrected by the value of 15 µg/l for a blank solution

[b] Resulting absolute masses of γ-MnO_2 dissolved in 2.0 ml of sample solution

[c] Relative to theoretical value of 308 mA h/g for the one-electron reduction of MnO_2

In accordance with an earlier suggestion [21], it is proposed that barium manganates(III) precipitate upon reductive formation of dissolved manganate(III) from γ-MnO_2. In the second voltammetric sweep, essentially the same response as regards observed peak potentials is being detected. Signals attributable to the formation and subsequent reduction of δ-MnO_2 certainly do not show up in Ba^{2+}-saturated 9 M KOH electrolyte solution (Fig. 3a). However, such signals are obvious in the absence of additional metal ions (see Fig. 2a and note [14]). These findings based on abrasive stripping voltammetric data strongly support previous X-ray diffractometric results [21], which revealed that no Mn_3O_4 was generated in RAM™ cells even after prolonged cycling when $BaSO_4$ had been added to the γ-MnO_2 cathode.

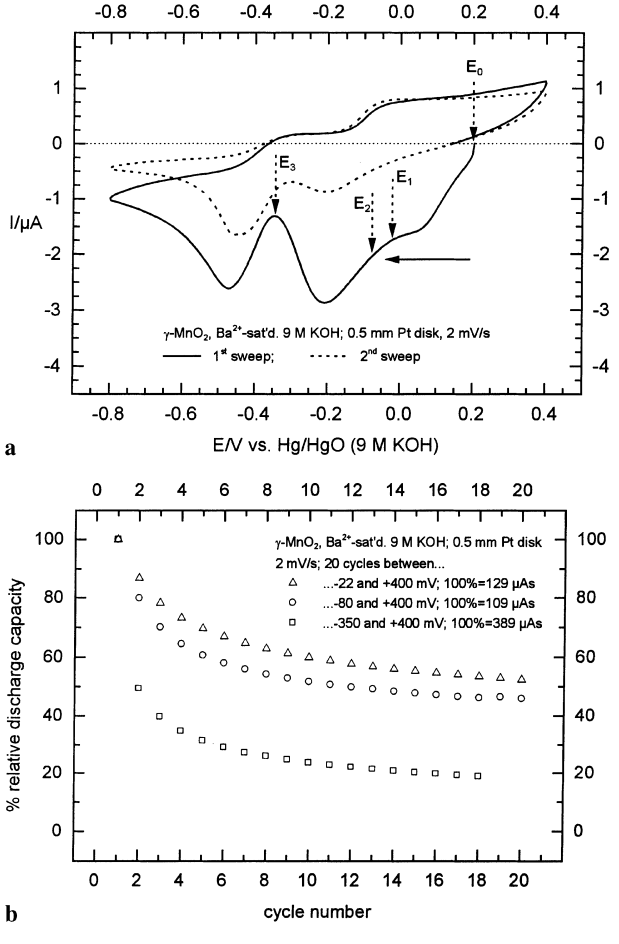

Fig. 3 **a** Cyclic abrasive stripping voltammetry of γ-MnO_2. Scan direction is indicated by *solid arrow*. Rest potential E_0 and various switching potentials E_1 to E_3 are indicated by *dotted arrows*. **b** Relative discharge capacity of γ-MnO_2 for various switching potentials as calculated from data sets analogous to that of Fig. 2c. Values corresponding to each 100% discharge capacity are indicated

Figure 3b shows relative discharge capacities of γ-MnO_2 in Ba^{2+}-saturated eletrolyte solutions following the procedure outlined above. Generally, enhanced reversibility of the one-electron reduction of γ-MnO_2 in the presence of Ba^{2+} ions is evident (see Fig. 2c). Moreover, the difference between 30% and 40% DOD is more pronounced than in plain 9 M KOH electrolyte solutions. These findings not only support the formation of barium manganates(III) during the process of reducing or discharging γ-MnO_2 in the presence of Ba^{2+} (see also [21]), but, more importantly, even during the very initial discharge steps, i.e., at 30 to 40% DOD, largely improved rechargeability is found which points towards a rapid formation of reversibly oxidizible barium manganates(III) even under these conditions, where bulk dissolution of MnOOH is not yet expected.

The entire electrochemical activity of γ-MnO_2 is suppressed in the case of Zn^{2+}-saturated 9 M KOH electrolyte solution (Fig. 4a). From Eqs. 1 and 2, formation of insoluble and, other than in case of added Ba^{2+} ions, essentially electrochemically inactive Zn manganates(III) were proposed in order to explain the observed response [15]. Relative discharge capacities derived over 10 to 20 cycles under these conditions also reflect this behaviour (Fig. 4b). However, the time scale needed to come to these results is significantly reduced when employing AbrSV rather than low-scan rate methods at bulk electrodes [14].

A comparison of the reversibility of γ-MnO_2 at 40% DOD in 9 M KOH and in the presence of either Ba^{2+} or Zn^{2+} ions in such electrolyte solutions is presented in Fig. 5. Interestingly, at this DOD and in the presence of Zn^{2+} ions, the available capacity of γ-MnO_2 is not being reduced as much as under conditions of 100% DOD. However, from the trend of the data, it can be expected

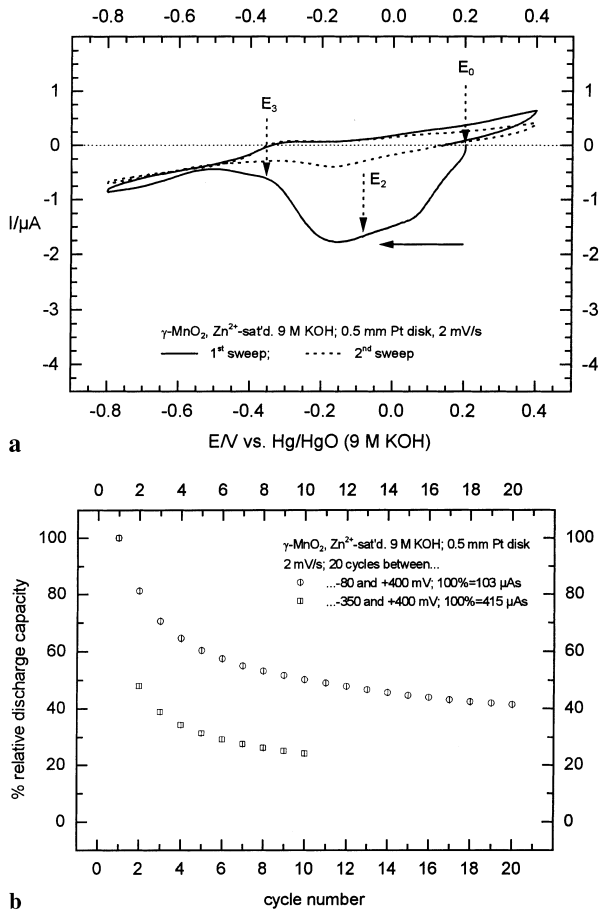

Fig. 4 **a** Cyclic abrasive stripping voltammetry of γ-MnO_2. Scan direction is indicated by *solid arrow*. Rest potential E_0 and switching potentials E_2 and E_3 are indicated by *dotted arrows*. **b** Relative discharge capacity of γ-MnO_2 for various switching potentials as calculated from data sets analogous to that of Fig. 2c. Values corresponding to each 100% discharge capacity are indicated

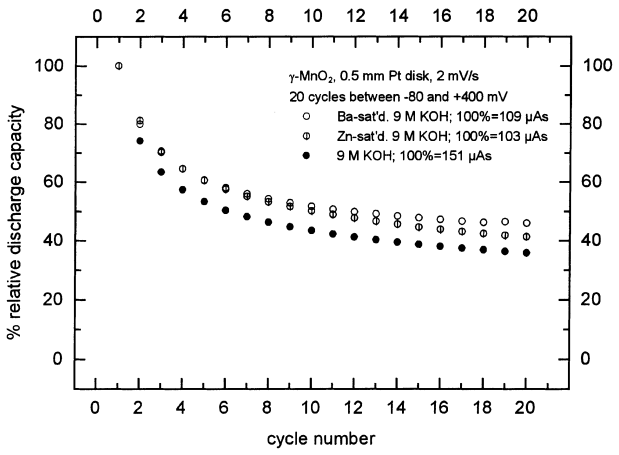

Fig. 5 Comparison of relative discharge capacity values of γ-MnO_2 in various electrolyte solutions under conditions of cyclic abrasive stripping voltammetry. Starting from rest potential E_0, switching potentials were −80 and 400 mV, respectively. Values corresponding to each 100% discharge capacity are indicated

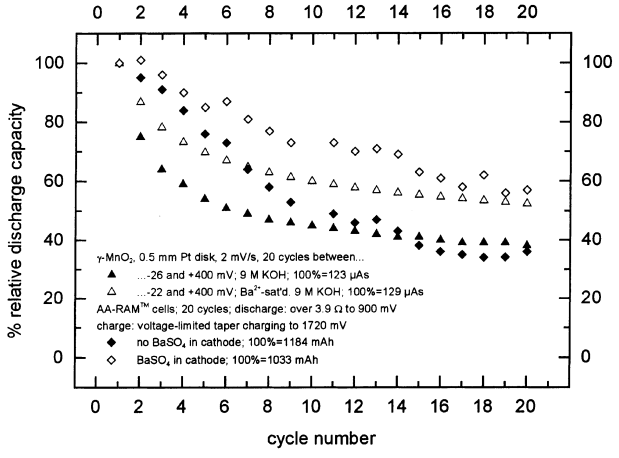

Fig. 6 Comparison of values of relative discharge capacity of γ-MnO_2 when derived from either cyclic abrasive stripping voltammetric or conventional discharge/charge experiments at AA-sized RAM cells. Values corresponding to each 100% discharge capacity are indicated (1 mA h = $3.6 \cdot 10^6$ μA s)

that, upon further cycling, the capacity of γ-MnO_2 would be reduced in the presence of Zn^{2+} relative to the case of no added metal ions. It can be concluded that formation of electrochemically inactive Zn manganates(III) is kinetically controlled ("ageing") and occurs to only a minor extent under conditions of high-rate discharge. The presence of Ba^{2+} ions improves and stabilizes the rechargeability of γ-MnO_2, as discussed above.

The method of AbrSV has thus been tested on previously known or proposed effects, such as the formation of barium or zinc manganates(III) in the presence of Ba^{2+} or Zn^{2+} ions in the electrolyte solution. The results clearly show that this still young method is able to provide additional and supporting evidence for such proposals on a greatly reduced time scale when compared to results of more conventional testing methods on bulk electrodes [5, 14]. Future work has to show whether AbrSV can even be applied to predict properties of battery electrode materials.

Finally, the relative discharge capacities at 30% DOD under conditions of AbrSV are compared with those derived from AA-sized RAM^{TM} cells (Fig. 6). This comparison is understood to be qualitative, since AbrSV cycling of γ-MnO_2 represents conditions of high-rate 30% discharge, while that of AA cells is a medium- to low-rate 50% discharge [8]. AA cells are conventionally discharged across a constant ohmic load ($R = 3.9\ \Omega$) to 900 mV and subsequently charged by the voltage-limited taper charging method to 1720 mV cell voltage [7, 8].

In the approach described in this paper, the DOD in the AbrSV sense was varied at constant voltammetric scan rate in order to check for any comparability of resulting relative discharge capacity characteristics with those of RAM^{TM} cells. As already discussed, the particle size was not found to significantly affect the AbrSV response in the case of the γ-MnO_2 used. Alternatively,

one could, of course, further elaborate on a variation of scan rate. In the author's experience, lower scan rates do not improve the resolution of voltammetric signals, and, with the chosen electrode, one quickly reaches the domain of background current. At voltammetric scan rates higher than 2 mV/s, the ohmic iR drop due to the resistance of the material itself leads to severe distortion of resulting voltammograms.

However, from the measured relative discharge capacity traces it can be deduced that a reduced DOD in AbrSV studies compensates for the high-rate discharge conditions at the chosen voltammetric scan rate of 2 mV/s, and AbrSV data show the same trend as conventional cycling results of AA-sized cells. From the 10th cycle onwards, essentially the same relative discharge capacity values are found under either set of discharge conditions and in the presence or absence of Ba^{2+} ions in the electrolyte solutions. The time necessary to complete the AbrSV experiment shown amounts to 2.7 h, which is to be compared with about 360 h it takes for a similar experiment under conditions of conventional testing methods.

Conclusions

Abrasive stripping voltammetry has been shown to be a valuable method in the field of battery electrode material research. The reversibility of the first one-electron reduction step of γ-MnO_2, which is successfully being taken advantage of in rechargeable alkaline manganese dioxide cells, was confirmed to be substantially enhanced in the presence of Ba^{2+} ions in 9 M KOH electrolyte solutions, while Zn^{2+} ions were found to suppress this reversibility. Conditions were evaluated which allow for the direct comparison of data trends from AbrSV experiments with those from conventional testing of AA-sized RAM^{TM} cells. Accordingly, AbrSV leads to an approximately 130-fold reduced time scale for such investigations, and is consequently recommended to be more generally tested as an alternative to conventional methods of testing and screening battery electrode materials.

Acknowledgements The continuous and generous support of Professors J. O. Besenhard and K. Kordesch is most gratefully acknowledged. The Austrian 'Fonds zur Förderung der wissenschaftlichen Forschung' provided financial support through project No. M 00383-CHE. Stimulating discussions with Dr. J. H. Albering, Dr. R. Andreaus, Dr. L. Binder, B. Evers, I. Schneider and Dr. W. Taucher-Mautner initiated this study. Batteries were prepared and tested by S. Šimić. We thank M. Zischka of the Institut für Analytische Chemie of the Technische Universität, Graz, for carrying out inductively coupled plasma analyses.

References

1. Scholz F, Nitschke L, Henrion G (1989) Naturwissenschaften 76: 71
2. Scholz F, Nitschke L, Henrion G, Damaschun F (1989) Fresenius Z Anal Chem 335: 189
3. Scholz F, Lange B (1992) Trends Anal Chem 11: 359
4. Scholz F, Lange B (1994) Chem Soc Rev 23: 341
5. Fiedler DA, Besenhard JO, Fooken MH (1997) J Power Sources 69: 11
6. Binder L, Jantscher W, Fiedler DA, Kordesch KV (1997) In: Holmes CF, Landgrebe AR (eds) Batteries for portable applications and electric vehicles, PV 97–18. The Electrochemical Society, Orlando, pp 583–591
7. Kordesch K, Tomantschger K, Daniel-Ivad J (1995). In: Linden D (ed) Handbook of batteries. McGraw-Hill, New York, pp 34.1–34.12
8. Kordesch K, Weissenbacher M (1994) J Power Sources 51: 61
9. Kozawa A (1974) In: Kordesch K (ed) Batteries, vol I. pp 385–519
10. Qu DY, Conway BE, Bai L, Zhou YH, Adams WA (1993) J Appl Electrochem 23: 693
11. Qu DY, Bai L, Castledine CG, Conway BE, Adams WA (1994) J Electroanal Chem 365: 247
12. Fiedler DA, Besenhard JO (1997) In: Holmes CF, Landgrebe AR (eds) Batteries for portable applications and electric vehicles, PV 97-18. The Electrochemical Society, Orlando, pp 893–904
13. McBreen J (1975) Power Sources 5: 525
14. McBreen J (1975) Electrochim Acta 20: 221
15. McBreen J (1975) In: Kozawa A, Brodd RJ (eds) Manganese dioxide symposium, vol. I. The Electrochemical Society, Cleveland, pp 97–110
16. Swinkels DAJ, Anthony KE, Fredericks PM, Osborn PR (1984) J Electroanal Chem 168: 433
17. Hong Z, Zhenhai C, Xi X (1989) J Electrochem Soc 136: 2771
18. Chabre YP (1991) J Electrochem Soc 138: 329
19. Swinkels DAJ (1992) Prog Batter Batter Mater 11: 97
20. Chabre YP, Pannetier J (1995) Prog Solid State Chem 23: 1
21. Albering JH, Weissenbacher M, Reichmann K, Besenhard JO, Kordesch K (1995) Z Kristallogr Suppl 9: 56